International Journal of Nanomedicine Dovepress

Open Access Full Text Article ORIGINAL RESEARCH

Antimicrobial Effects of Thonningianin a (TA)-Loaded Chitosan Nanoparticles Encapsulated by a PF-127 hydrogel in Diabetic Wound Healing

Qian Lin[1,*], Fucheng Zhu[1,*], Aji Shiye[1,*], Runyu Liu[1,2], Xiaolan Wang[1], Zi Ye[1], Yinhuan Ding[3], Xiaolei Sun[1,4–8], Yarong Ma[9]

[1]Department of General Surgery (Vascular Surgery), the Affiliated Hospital of Southwest Medical University, Luzhou, 646000, People's Republic of China; [2]Department of Hepatobiliary Pancreatic Vascular Surgery, the Second Affiliated Hospital of Chengdu Medical College, Chengdu, 610057, People's Republic of China; [3]Department of Laboratory Medicine, the Affiliated Hospital of Southwest Medical University, Sichuan, 646000, People's Republic of China; [4]Department of Interventional Medicine, the Affiliated Hospital of Southwest Medical University, Luzhou, 646000, People's Republic of China; [5]Laboratory of Nucleic Acids in Medicine for National High-Level Talent, Nucleic Acid Medicine of Luzhou Key Laboratory, Southwest Medical University, Luzhou, 646000, People's Republic of China; [6]Key Laboratory of Medical Electrophysiology, Ministry of Education & Medical Electrophysiological Key Laboratory of Sichuan Province, Collaborative Innovation Center for Prevention and Treatment of Cardiovascular Disease of Sichuan Province, Institute of Cardiovascular Research, Southwest Medical University, Luzhou, 646000, People's Republic of China; [7]Cardiovascular and Metabolic Diseases Key Laboratory of Luzhou, Luzhou, 646000, People's Republic of China; [8]School of Cardiovascular Medicine and Sciences, King's College London British Heart Foundation Centre of Research Excellence, Faculty of Life Science and Medicine, King's College London, London, SE5 9NU, UK; [9]Department of Ophthalmology, the Affiliated Hospital of Southwest Medical University, Luzhou, 646000, People's Republic of China

*These authors contributed equally to this work

Correspondence: Xiaolei Sun; Yarong Ma, Email sunxiaolei@swmu.edu.cn; sunxiaolei_lg@163.com; mayarong_88@163.com

Background and Purpose: Diabetic wounds are serious chronic complications of diabetes and can lead to amputation and death. Although considerable progress has been made in drugs and materials for treating it, it's still an urgent clinical problem as the materials and drugs have potential therapeutic drawbacks, such as low delivery efficiency and poor tissue permeability. To promote diabetic wound healing, a composite of thonningianin A (TA)-loaded chitosan nanoparticles (CNPS) encapsulated by a Pluronic F-127 (PF-127) hydrogel (TA-CNPS-PF) was developed in this study.

Methods: TA-CNPS was prepared by ionic gelation method and TA-CNPS was thoroughly dispersed into PF-127 hydrogel to prepare TA-CNPS-PF. The particle size, hydrogel structure, encapsulation ratio, release ratio, antimicrobial properties of TA-CNPS-PF were determined and the effect of TA-CNPS-PF on diabetic wounds was assessed. The effect of TA on macrophage polarization was also examined in vitro.

Results: The particle size was approximately 100 nm of TA-CNPS-PF and the hydrogel had a homogeneous three-dimensional reticulation structure. The encapsulation efficiency of TA in the CNPS were 99.3% and the release ratio of TA-CNPS-PF was approximately 86% and has antimicrobial properties. TA-CNPS-PF promoted diabetic wound healing significantly. Histopathology confirmed that TA-CNPS-PF promoted complete re-epithelialization and adequate collagen deposition. TA promoted the polarization of M1 macrophages into M2 macrophages via light microscopy, immunocytometry and flow cytometry. TA-CNPS-PF also promoted an increase in the number of M2 macrophages in diabetic wounds.

Conclusion: TA promotes diabetic wound healing by promoting the polarization of M1 macrophages into M2 macrophages and TA-CNPS-PF has good antimicrobial activity and a good drug release ratio in this study, which provides a new direction for the treatment of diabetic wounds and is expected to be highly advantageous in clinical diabetes wound therapy.

Keywords: thonningianin A. TA, TA nanoparticle hydrogel, TA-CNPS-PF, diabetic wound, M1 macrophages, M2 macrophages

Introduction

Diabetes mellitus (DM) is a chronic metabolic disorder of the endocrine system characterized by elevated blood glucose levels.[1] It is one of the most common and fastest growing diseases in the world.[2] Wound healing is a serious complication

Received: 22 July 2024
Accepted: 12 November 2024
Published: 3 December 2024

Graphical Abstract

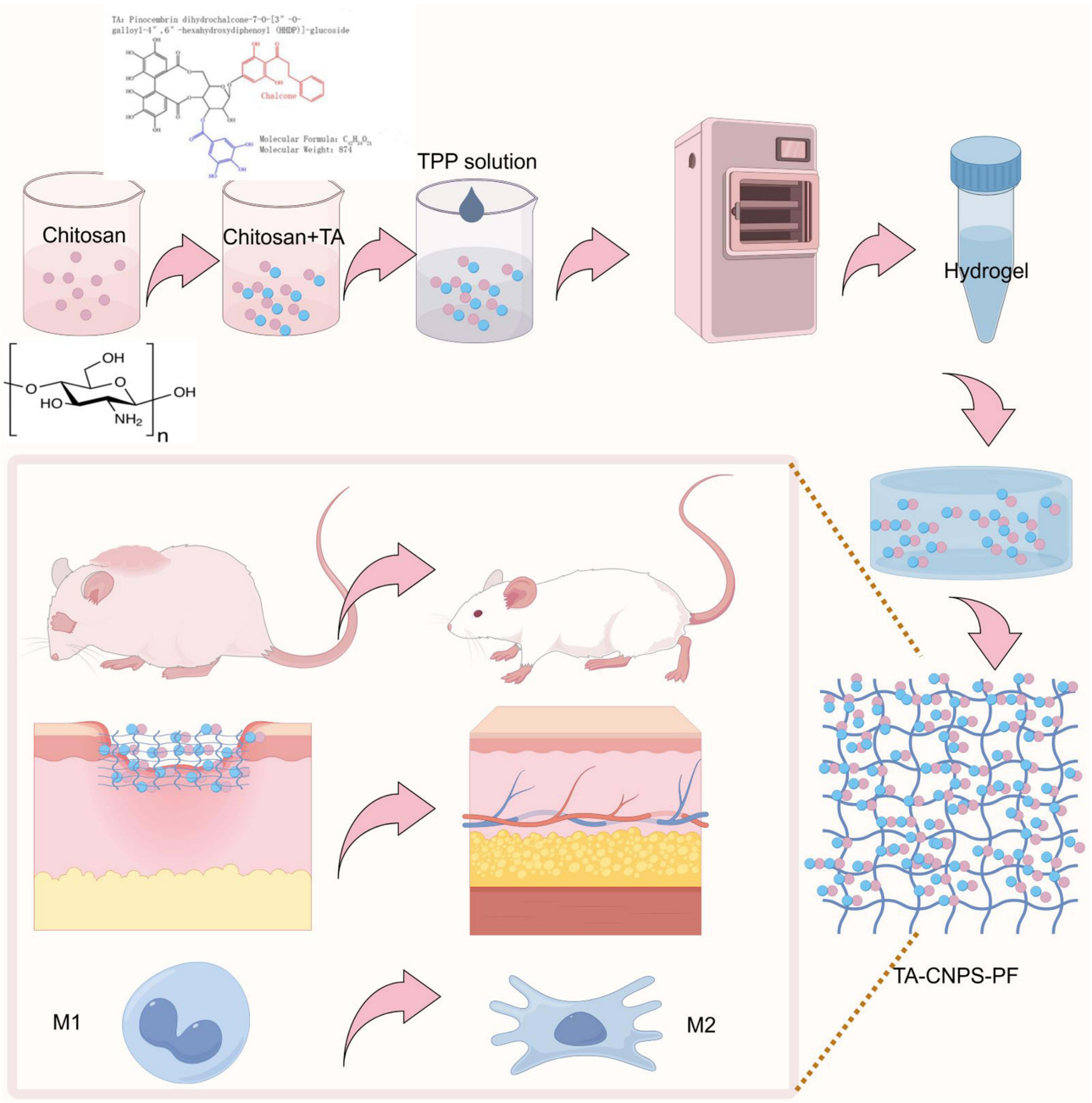

in diabetic patients, and it has become a substantial issue for both patients and the public health system.[3] Approximately 2.5–12% of the world's health budget is spent annually on individuals with diabetes, and diabetic wounds account for the majority of these cases.[4] Prolonged difficult-to-heal wounds may develop into foot ulcers and even lead to foot amputation and death.[5] Therefore, there is still an urgent need to develop an effective therapeutic strategy to ameliorate difficult-to-heal diabetic wounds.

Physiologically, wound healing is a dynamic and complex process that manifests in four successive phases: hemostasis, inflammation, proliferation and tissue remodeling.[6] During wound healing, the inflammatory phase is characterized by the production of various proinflammatory and chemokine factors, which lead to the infiltration of neutrophils and macrophages at

the site of injury.[7] The proliferative phase is characterized by the proliferation, migration and reorganization of fibroblasts and vascular endothelial cells to form granulation tissue, collagen, and neovascularization and ultimately the formation of a large amount of extracellular matrix (ECM), which accelerates wound healing.[8] At the site of the wound, macrophages stimulate angiogenesis, fibroproliferation and ECM production and play important bridging roles in the transition of the wound from the inflammatory to the proliferative phase. During the inflammatory response in wounds, macrophages converge and differentiate into proinflammatory macrophages (M1) and anti-inflammatory macrophages (M2).[9] M1 macrophages produce proinflammatory mediators such as TNF-α, IL-1, IL-6, and protease matrix metalloproteinases, whose main function is to promote inflammatory responses and fight pathogens during the inflammatory phase, but they often exacerbate tissue damage when they overaccumulate. M2 macrophages mainly participate in the downregulation of inflammation by releasing anti-inflammatory factors such as IL-4, IL-10, and IL-13 while secreting VEGF, EGF and TGF to promote cell proliferation, granulation tissue formation, angiogenesis and wound healing.[10] Chronic diabetic wounds are in the inflammatory phase for a long period of time and overaccumulate M1 macrophages, which are difficult to polarize into M2 macrophages. This is one of the main reasons why diabetic wounds fail to heal. Thus, promoting the polarization of M1 macrophages to M2 macrophages is beneficial for accelerating diabetic wound healing.[11]

Thonningianin A (TA) is a novel monomeric compound extracted from the Chinese medicinal herb *Penthorum chinense* Pursh. In the previous research, TA was identified and isolated via human umbilical vein endothelial cell membrane solid-phase chromatography combined with ultrahigh-performance liquid chromatography-time-of-flight mass spectrometry [UHPLC-(Q)TOF-MS]. TA can inhibit the expression of oxidative stress-associated inflammasome-related NLRP3 in the aortic arteries of patients with atherosclerosis.[12] However, it is unclear whether the role of TAs in the inflammatory response is beneficial for diabetic wound healing.

Chitosan (CS) is a naturally occurring polymeric polysaccharide that is soluble in acidic solutions and contains reactive amino and hydroxyl functional groups with cationic properties, thus displaying unique chelating, film-forming, and polycationic properties.[13–15] Chitosan also has good hemostatic, antimicrobial, biocompatible and biodegradable properties.[16] Controlled or sustained nanoparticle drug delivery systems enable the maintenance of a constant drug concentration at the desired site.[17] Maintaining a constant drug concentration at the desired site is essential for diabetic wound treatment. The preparation of nanoparticles from chitosan has been shown to improve drug stability, thereby increasing drug accumulation.[18] The role of chitosan nanoparticles in promoting wound healing has been demonstrated.[19] Therefore, the encapsulation of TA into chitosan nanoparticles for wound treatment facilitates the release of TA in a controlled manner, maintains a constant concentration of TA in the wound and improves the stability and utilization of TA.

Pluronic F-127 (PF-127), a synthetic copolymer composed of polyethylene-polypropylene glycol, has unique thermoreversible properties. PF-127 is a liquid at low temperatures and gradually transforms into a semisolid gel at high temperatures. It has been extensively studied in the literature as a drug carrier.[20–22] Owing to the reversible thermoresponsive behavior of PF-127, it can adapt to the complex and irregular space of diabetic wounds, allowing the bioactive agent to adhere to the target site and exert its biological effects.[23] In addition, PF-127 is biocompatible, has low toxicity and can be efficiently loaded with drugs without reacting chemically.[24] Hydrogels encapsulated with nanoparticles are effective systems that maintain a humid environment and promote the rapid healing of wounds.[16] PF-127 is an ideal carrier for drug formulation. The dispersion of TA-loaded chitosan nanoparticles into the PF-127 hydrogel for diabetic wound treatment enables this material to adapt to the different spatial structures of diabetic wounds, keep the wound moist, promote uniform release of TA into the wound and provide better conditions for diabetic wound healing.[17]

In this work, the preparation of TA-CNPS-PF was first described in detail, and the characterization, antimicrobial properties and therapeutic effects of TA-CNPS-PF on the polarization of M1 macrophages into M2 macrophages for diabetic wound healing were investigated via in vivo and in vitro experiments.

Materials and Methods

Materials

Chitosan (CS, deacetylation degree ≥95%, viscosity 100–200 MPa/s) (C105799-2.5 kg) was purchased from Aladdin (Shanghai, China). Acetic acid aqueous solution (1%) (BQS116462-500 mL) was purchased from Qisong (Beijing, China). Sodium

hydroxide solution (NaOH, c=2 mol/L) (SLT-E11D1GAS) was purchased from BOLINDA (Shenzhen, China). Sodium tripolyphosphate (TPP) (238503) was obtained from Sigma–Aldrich Corp. (St. Louis, MO, USA). Pluronic(R) F-127 (P2443-250G) was purchased from Sigma–Aldrich Corp. (St. Louis, MO, USA). Phosphate-buffered saline (PBS, pH 7.4) (C10010500BT) was purchased from Gibco (Carlsbad, CA, USA). Thonningianin A, pinocembrin dihydrochalcone-7-O-[3″-ogalloyl-4″6″-hexahydroxydiphenyl]-glucoside (TA), was obtained from Push Biotechnology, Chengdu, China. *Escherichia coli* (*E. coli* ATCC® 25922™) and *Staphylococcus aureus* (*S. aureus* ATCC® 25923™) from the Microbiology Group, Department of Laboratory Medicine, Southwest Medical University, China. Sprague–Dawley rats were purchased from the Animal Experiment Centre of Southwest Medical University. Synergy Bio 60% fat feed (D12492) was purchased from Synergy Pharmaceutical Bioengineering (Jiangsu, China). Sodium citrate buffer (0.1 mol/L, pH 4.5, sterile) (C1013-100 mL) was purchased from Solarbio (Beijing, China). Streptococcus aureus (STZ) (S8050–100 mg) was purchased from Solarbio (Beijing, China). A blood glucose test strip (EZ3-200) was purchased from Call (Hangzhou, China). A Masson stain kit (G1346-8) was purchased from Solarbio (Beijing, China). RAW264.7 cells (CL-0190) were purchased from Procell (Wuhan, China). Fetal bovine serum (FBS) (AC03L055) was purchased from Life-ilab (Shanghai, China). Penicillin–streptomycin-amphotericin B (C0224-100 mL) was purchased from Beyotime (Shanghai, China). DMEM (C11885500BT) was purchased from Gibco (Carlsbad, CA, USA). A CCK8 kit (CK04) was purchased from DOJINDO (Shanghai, China). 4% paraformaldehyde (P1110-500 mL) was purchased from Solarbio (Beijing, China). Triton X-100 (T8787) was purchased from Sigma–Aldrich Corp. (St. Louis, MO, USA). Bovine serum albumin (BSA) (A1933-1G) was purchased from Sigma–Aldrich Corp. (St. Louis, MO, USA). CD86 monoclonal antibody (942-MSM1-P0) was purchased from Invitrogen (Carlsbad, CA, USA). Anti-Mannose Receptor/CD206 antibody (ab64693) was purchased from Abcam (Cambridge, UK). The donkey anti-rabbit IgG (H+L) highly cross-adsorbed secondary antibody Alexa Fluor™ 555 (A31572) was purchased from Invitrogen (Carlsbad, CA, USA). The donkey anti-mouse IgG (H+L) highly cross-adsorbed secondary antibody Alexa Fluor™ 488 (A21202) was purchased from Invitrogen (Carlsbad, CA, USA). The APC-conjugated anti-mouse CD206/MMR antibody (E-AB-F1135E) was purchased from Elabscience (Wuhan, China). An anti-fluorescence quenching encapsulant (containing DAPI) (P0131-25 mL) was purchased from Beyotime (Shanghai, China).

Preparation of TA-CNPS-PF

Preparation of TA Nanoparticles (TA-CNPS)

TA nanoparticles were prepared using chitosan as a carrier. A total of 45 mg of chitosan was slowly added to 15 mL of acetic acid (1 wt%) (600 rpm until dissolution),[16] and 2 mol/L NaOH was used to adjust the pH of the chitosan solution to 5~6; 2 mg/mL TA working solution was added (TA was dissolved in a solvent of PEG400: saline: anhydrous ethanol = 6:3:1), and X mL of the TA (depending on the weight of the SD rats at the time of STZ injection, the average weight of the rats in the group was taken) was mixed with the chitosan solution and stirred (Based on the pre-experimental results in Supplementary Figure 1, the concentration used in this research was 0.6 mg/Kg in vivo); 15 mL of 0.1% TPP solution was prepared with distilled water and slowly added dropwise (40 drops/min, the solution appeared as a milky white suspension) into the above TA-chitosan solution and was centrifuged at 1000 rpm for 30 min. The supernatant was transferred to a new tube and stored for subsequent analysis, and the formed pellet was washed three times in dd-water. The samples were freeze-dried at −80 °C for 72 hours. The mixture was stored at −20 °C in the dark.

Preparation of the TA Nanoparticle Hydrogel (TA-CNPS-PF)

Temperature-sensitive PF-127-embedded TA nanoparticles were prepared by dissolving PF-127 in distilled water with magnetic stirring to form a clarified solution (20%, w/v). TA nanoparticles were thoroughly dispersed into the clarified solution of PF-127 under magnetic stirring at 4 °C to prepare a hydrogel loaded with TA-CNPS.

TA Nanoparticle Hydrogel Characterization Assay

TA-CNPS Particle Size and Hydrogel Characterization

Scanning electron microscopy was used to detect the particle size of the TA nanoparticles and the hydrogel structure of the TA nanoparticles, and the samples were sent to Chengdu Rilai Biotechnology Co. Ltd.[25]

Measurement of the TA Nanoparticle Encapsulation Ratio via UV Spectrophotometry

Five different concentrations of TA were prepared by dissolving TA in DMSO. The absorption spectra of TA were measured and plotted via capillary electrophoresis to determine the maximum absorption wavelength of TA. The absorbance (A) of the five different concentrations of TA was measured at the 230nm and the standard curve was plotted. The absorbance of the supernatant to be tested was measured at 230nm and the amount of TA in the supernatant was determined from the standard curve. According to the following equation:

Encapsulation ratio (%) = (1 - (total TA content in the supernatant/initial TA content)) × 100%.

In vitro Release Ratio of TA Nanoparticle Hydrogels via UV Spectrophotometry

The TA nanoparticle hydrogel was fully dissolved in deionized water and placed in a dialysis bag, which was put into PBS containing 0.5% Tween-80 and continuously shaken in a 37 °C constant-temperature water-bath shaker, after which 3 mL of the liquid was removed at regular intervals and replenished with an equal amount of PBS. The absorbance of the taken liquid was measured with a UV spectrophotometer to calculate the amount of TA released at a certain time. The release rate of the drug was calculated according to the following formula: release ratio (%) = $C_t/C_0 \times 100\%$, where C_0 represents the concentration of TA in the supernatant at t=0 and Ct represents the concentration of TA in the supernatant at a specific time.

In vitro Antimicrobial Properties

Weighed tryptone (No. HB4114), added to distilled water and heated with stirring to dissolve. Then added agar (No. HB8274) and heated again with stirring until dissolved. Dispensed the medium into petri dishes, allowed to solidify and then autoclaved at 121°C for 20–30 minutes before use. *Escherichia coli (E. coli ATCC® 25922™)* and *Staphylococcus aureus (S. aureus ATCC® 25923™)* were calibrated in sterile liquid medium to a 0.5 McClatchy turbidimetric standard ($1x10^8$ CFU /mL). Bacteria were uniformly distributed on the surface of Soybean Casein Digest Agar (TSA) using a microbial applicator (Model: XK) and 1.5 cm diameter samples (saline, PF, CNPS-PF, TA-CNPS-PF) sterilized by UV light for 15 min were placed in the center of the petri dish, which were incubated at 37 °C under aerobic conditions. The area of the zone of inhibition was measured via lmage J. Three parallel samples were used for each experiment.[16]

Animal Study

Sprague-Dawley Rat Experiment

Seven-week-old Sprague–Dawley rats weighing approximately 200 g were selected for the wound healing experiments. All animal experimental procedures were performed in accordance with protocols approved by the Animal Care and Use Committee of Southwest Medical University (No. 20231030–001) and laboratory animal administration rules of China. The rats were housed in the Laboratory Animal Center of Southwest Medical University at a temperature of 25 °C, a humidity of 50–60% and 12 h of alternating light and dark environments for free access to food and water, and the experiments were conducted after 1 week of acclimatization.

Establishment of an Animal Model of Type 2 Diabetes Mellitus

Twenty rats were randomly divided into a control group (n=5) and a model group (n=15). In the model group, the rats were fed high-fat and high-sugar diets for 4 weeks. Then each rat was given 30 mg/kg of 1% streptozotocin solution (dispensed within half an hour in an ice bath protected from light) by intraperitoneal injection for 4 consecutive days before being fasted for 12 h. Random blood glucose was monitored continuously on 0, 2, 3, 4, 5, 6, 7, 14 d. Rats with random blood glucose levels ≥16.7 mmol/L and those with excessive drinking, food, urination, yellowish fur, reduced activity and decreased body mass were considered to be successful in the model of type 2 diabetes mellitus. The 15 rats were fed a high-fat and high-sugar diet for 2 weeks, and a diabetic trauma model was established.[26]

Trauma Modeling

After anesthesia with isoflurane, the dorsal midline area 0.5 cm below the clavicle on the back of each rat was selected, the skin was prepared and disinfected, and a circular full-layer skin injury wound was made with a 2 cm diameter skin punch. The diabetes model group was randomly divided into Groups B, C and D. The wounds in Group B were treated

with 200 μL of saline, the wounds in Group C were treated with 200 μL of hydrogel containing chitosan nanoparticles, and the wounds in Group D were treated with 200 μL of TA-containing chitosan nanoparticles. Group A (the control group) was prepared via the same method for full skin injury wounds with 200 μL of saline.

Wound Healing Ratio

The wound dressings were changed every two days and photographs were taken at 3, 7 and 14 days. The wound area was traced and measured by ImageJ. The wound healing ratio was used as an index for evaluating wound healing. The experimental animals were sacrificed after 14 days.

Wound healing ratio (%) = (initial wound area - current wound area/initial area) × 100%.

Histological Study

On Days 7 and 14, whole skin tissues were removed within 5 mm of the trauma margin after photographs of the trauma were taken. Fresh tissues were cleaned and placed directly in OCT embedding agent and frozen directly at −80 °C. The prepared frozen tissues were cut into 5-μm-thick sections via a cryostat for subsequent hematoxylin–eosin (HE) staining and Masson's trichrome staining. Microscopy image analysis of the area of inflammatory cell infiltration and the formation of collagen fibers in each group were performed via K-viewer software.

Immunofluorescence

Rat skin tissues were selected for immunofluorescence on Day 7 after trauma induction. Skin tissues with a thickness of 5 μm were fixed, permeabilized, closed and incubated with an anti-CD206 primary antibody overnight at 4 °C, followed by incubation with the corresponding fluorescent dye-coupled secondary antibody. DAPI was used to stain the nucleus. Finally, an immunofluorescence microscope (Olympus BX53, Japan) was used for observation.

Cell Culture

RAW264.7 Culture

RAW264.7 cells were cultured in 10% fetal bovine serum (FBS), 100 U/mL penicillin, 0.1 mg/mL streptomycin and 0.25 μg/mL amphotericin B in DMEM at 37 °C in a 5% CO_2 thermostatic cell culture incubator (Thermo Scientific Forma Steri-Cycle i160).

Diabetic Macrophage Model

RAW264.7 cells were cultured in medium supplemented with 10% fetal bovine serum (FBS), 100 U/mL penicillin, 0.1 mg/mL streptomycin, 0.25 μg/mL amphotericin B and DMEM supplemented with 40 mmol/L glucose. RAW264.7 cells were subsequently cultured at 37 °C in 5% CO_2 to construct a diabetic cell model.[27]

TA in vitro Cytotoxicity Assay

First, a RAW264.7 cell suspension was prepared for counting, 3×10^3 cells were inoculated into a 96-well plate with approximately 100 μL of cell suspension per well, and the same samples were performed in 6 replicates. Then, different concentrations of TA were added to the wells at 0, 1, 2.5, 5, 10 and 20 μM, and the cells were cultured at 37 °C in a 5% CO_2 incubator for 24 h. Then, 10 μL of CCK8 was added, and the mixture was cultured for 2 h. The absorbance was measured at 450 nm, and the IC_{50} was calculated to determine the TA concentration.

Immunocytochemistry

After RAW264.7 cell species creep was observed, the control group, diabetes group, diabetes + TA group and TA group were established. The cells were fixed with 4% paraformaldehyde, permeabilized with 0.1% Triton X-100, blocked with 5% BSA, incubated overnight with primary antibodies at 4 °C, incubated with secondary antibodies at room temperature, and subjected to DAPI staining, after which photographs were taken via immunofluorescence microscopy (Olympus BX53, Japan).

Flow Cytometry

After RAW264.7 cells were seeded on plates, the control group, diabetes group, diabetes + TA group and TA group were established. After cell treatment and counting, the cells were centrifuged at 1000 rpm for 5 min, washed with PBS containing 2% BSA, fixed with 4% paraformaldehyde at room temperature, resuspended with a membrane-breaking agent, added to a 1.5 mL EP tube at approximately 1×10^6/tube in a volume of 100 μL/tube, and incubated with an APC-conjugated anti-mouse CD206/MMR antibody. The cells were washed repeatedly and then tested (ACEA NovoCyte^{TM}2070).[28]

Statistical Analysis

All the data were acquired from ≥ 3 independent experiments and are expressed as the mean ± standard deviation (s.d). Prism 10.1.2 software was used for statistical analysis. A *t* test was used for comparisons of one condition between two groups, Tukey's multiple comparisons test was used for multiple groups, and $P < 0.05$ was considered statistically significant throughout the study.

Results

Characterization and Antibacterial Properties of TA Nanoparticle Hydrogels

Figure 1A shows the appearance of the TA working solution and the appearance of saline, PF-127, lyophilized CNPS, CNPS-PF, lyophilized TA-CNPS and TA-CNPS-PF. Figure 1B shows the morphology of CNPS and TA-CNPS by scanning electron microscopy. CNPS and TA-CNPS were uniformly distributed in a spherical shape, which maintained the intact particle morphology without collapsing, and the particle size was approximately 100 nm. Figure 1C shows that the hydrogel had a homogeneous three-dimensional reticulation structure, which was conducive to the adsorption and retardation of the drug. The encapsulation efficiency and loading percentage of TA in the CNPS were 99.3%. The amount of TA released from the CNPS at 37 °C was concurrently measured, and the results are shown in Figure 1D. The release of TA was rapid, followed by slow release, with a total release rate of approximately 86% after 48 h of incubation at 37 °C in PBS. The drug in the TA nanoparticle hydrogel group was released slowly, which was beneficial for the drug to maintain a longer effect. To understand the antimicrobial performance of TA-CNPS-PF, we investigated its antimicrobial activity against gram-negative (*Escherichia coli E. coli*) and gram-positive (*Staphylococcus aureus S. aureus*) bacteria, and a circle of inhibition assay revealed that the TA nanoparticle hydrogel system significantly increased the inhibitory ranges of both *E. coli* and *S. aureus*, which had favorable antimicrobial performance (Figure 1E). Interestingly, our results also found that the hydrogel also inhibited the growth of gram-negative and gram-positive to a certain extent (Figure 1E).

In vivo Wound Healing Effect of TA-CNPS-PF

The effects of TA-CNPS-PF on wound healing in diabetic rats were investigated by characterization and pathology. A model of type 2 diabetes was established by a high-fat and high-sugar diet with streptozotocin intraperitoneally followed by trauma modeling and trauma dressing for protection with single-cage feeding. HE staining and Masson staining were performed after trauma at 0 d, 3 d, 7 d, and 14 d (Figure 2A). Twenty SD rats were fed an ordinary maintenance diet for 1 week, and the difference in blood glucose between the control group and the model group was not significant. The rats in the model group were fed high-fat and high-sugar feed for 4 weeks and then injected with STZ. Random blood glucose was measured at 2, 3, 4, 5, 6, 7 and 14 days after STZ injection. The results in Figure 2B indicated that rat model of type 2 diabetes mellitus was established. The body weights of the rats in the model group were significantly lower after 2 weeks of STZ injection, whereas the body weights of the rats in the control group were slightly greater after 2 weeks of saline injection. The blood glucose and body weight results indicated that the type 2 diabetes mellitus model was successful (Figure 2B). Figure 2C shows the overall morphology and wounds of the rats in the control group, diabetic group, diabetic+CNPS-PF group and diabetic+TA-CNPS-PF group at 0, 3, 7 and 14 days. The rats in the control group presented a shiny hair color, whereas the rats in the model group presented rough and yellowish hair after STZ injection. Compared with the wounds of the other groups, the TA-CNPS-PF wounds healed the fastest, and the

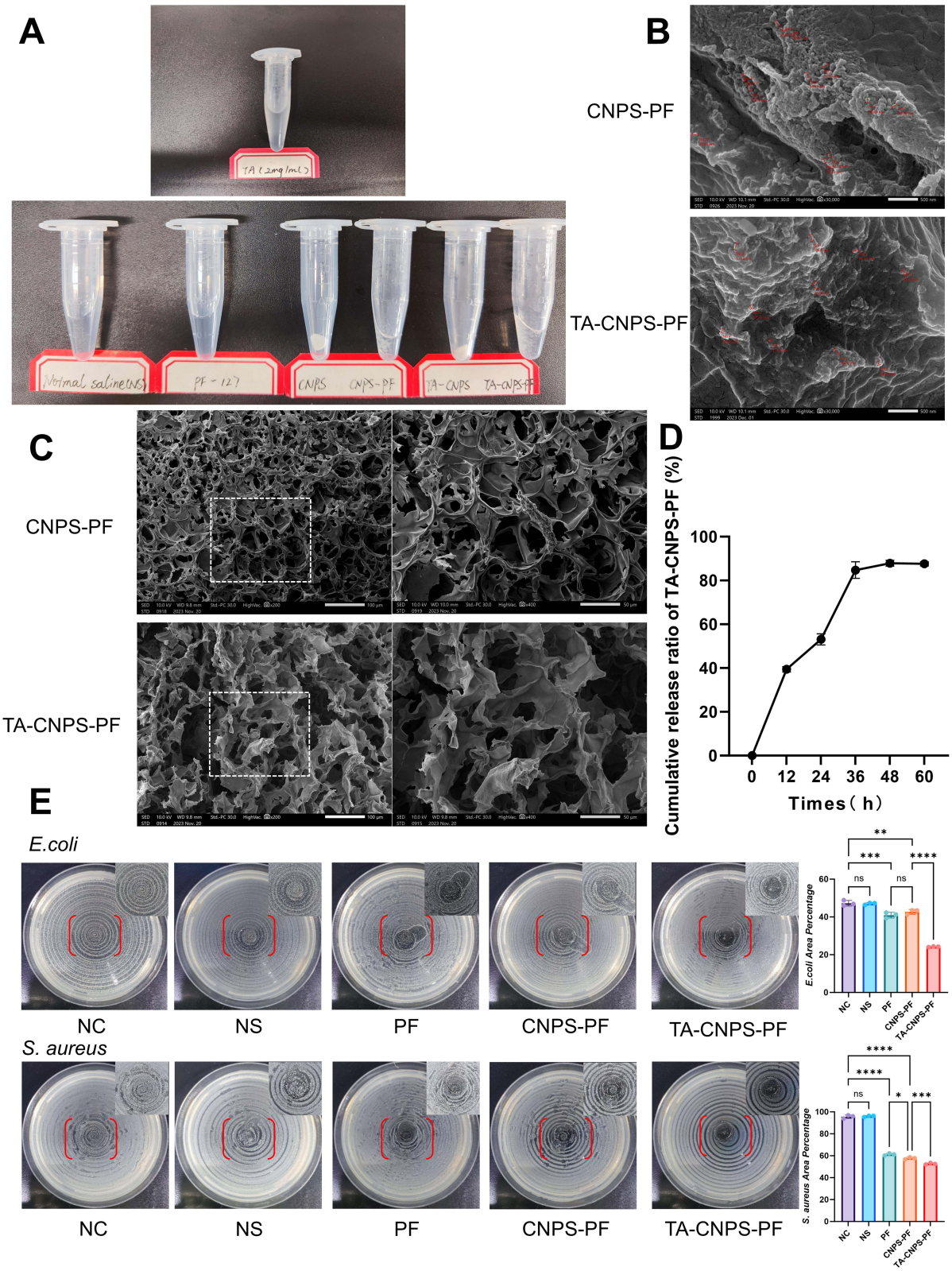

Figure 1 Characterization and antimicrobial properties of TA-CNPS-PF. (**A**) Appearance of the TA working solution and appearance of saline, PF-127, lyophilized CNPS, CNPS-PF, lyophilized TA-CNPS and TA-CNPS-PS; (**B**) Scanning electron microscopy image of the morphology of the CNPS, TA-CNPS and measured particle sizes (30,000× magnification, the red lines show the nanoparticles and measured size); (**C**) Scanning electron microscopy images of the morphology of the CNPS-PF and TA-CNPS-PF hydrogels (200× and 400×); (**D**) TA release behavior from TA-CNPS-PF at 37 °C (n = 3); (**E**) Control, saline, hydrogel, CNPS-PF and TA-CNPS-PF on *E. coli* and *S. aureus* inhibition zone images; TA-CNPS-PF had better in vitro antimicrobial properties (n = 3). Hydrogels also exhibit certain antibacterial abilities. *P < 0.05, **P < 0.01, ***P < 0.001, ****P < 0.0001.

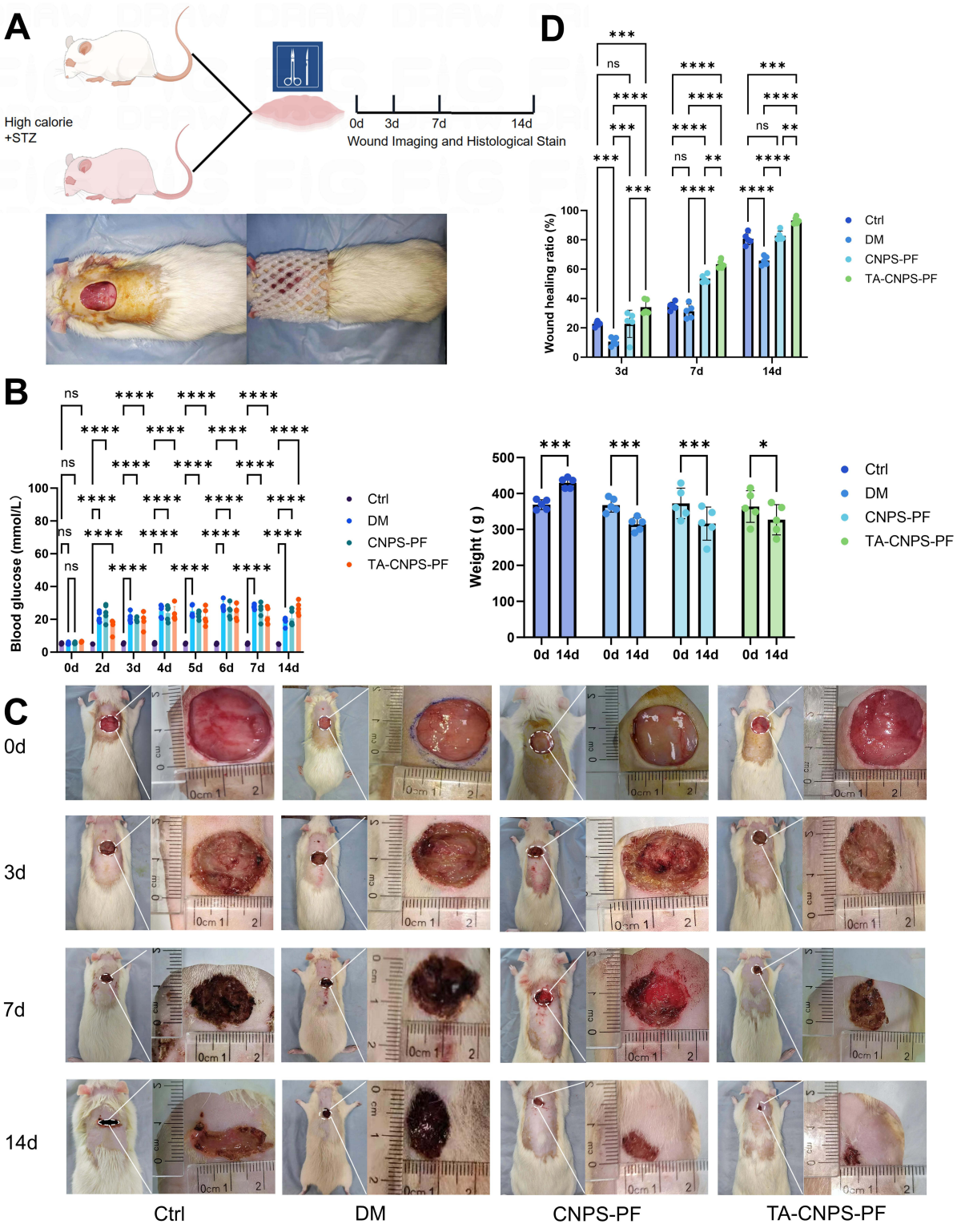

Figure 2 Wound healing efficacy of TA-CNPS-PF in vivo. (**A**) Flowchart of the animal experiment; (**B**) Random blood glucose and body weight data for each group of rats. A high-sugar and high-fat diet was fed for 4 weeks, and STZ (30 mg/kg) was intraperitoneally injected into the rats to establish a diabetes mellitus model. The random blood glucose levels of the rats in each group were measured at 0, 2, 3, 4, 5, 6, 7, and 14 days and the body weights of the rats in each group were measured at 0 and 14 days. According to the results, the random blood glucose level was greater than 16.7 mmol/L, and the body weight decreased significantly, whereas the blood glucose level in the control group did not change significantly, but the body weight increased at 14 d (n=5). (**C**) Macroscopic images of the whole body of rats in the control and diabetic groups and panoramic images of the healing of skin wounds in different treatment groups. One deep circular wound was produced in the skin of the back of each rat, d=2 cm, and was replaced with a new dressing at 3 d. The skin of the back of the rats had healed at 3, 7 and 14 d (n=5). (**D**) Quantitative analysis of the WHR of each group based on the wound area measured from the pictures taken at 0, 3, 7 and 14 d (n=5). *P<0.05, **P < 0.01, ***P < 0.001, ****P < 0.0001.

wound size was significantly reduced beginning at 3 d. The wound size had almost healed at 14 d. These results indicated that TA-CNPS-PF accelerated wound healing in diabetic rats. According to the quantitative analysis of wound size, the wound healing effect was significantly greater (WHR > 30%) in the diabetic + TA-CNPS-PF group than in the other three groups from 3 d (Figure 2D); the WHR reached approximately 95% at 14 d, which was greater than that of the control group, diabetic group, and diabetic + CNPS-PF group by 15% ($P = 0.0001$), 24.6% ($P < 0.0001$) and 12.8% ($P = 0.0013$) (Figure 2D). In summary, TA-CNPS-PF clearly demonstrated its effectiveness in promoting diabetic wound healing.

In vivo Histological Changes in TA-CNPS-PF at the Trauma Site

The results of HE and Masson staining of the skin tissues of the control and diabetic groups at 0 d revealed that the dermis and fat layer of the skin of the control group were thicker than those of the diabetic group. The collagen fibers in the dermis of the control group were more compact and regular than those in the dermis of the diabetic group. These findings confirmed the success of the model of type 2 diabetes mellitus in terms of histological evidence (Figure 3A). On Day 7, we collected skin tissues from the control group, diabetic group, diabetic+CNPS-PF group and diabetic+TA-CNPS-PF group and stained them with HE and Masson stains. Compared with the control group, the control group had wounds infiltrated with inflammatory cells, fewer neonatal capillaries, no epidermal shape, sparse collagen fibers and disordered arrangement. Compared with the control group, the diabetic group had wounds infiltrated with more inflammatory cells, a small number of scattered and isolated capillaries, no epidermal shape, sparse collagen fibers and disordered arrangement. Compared with the control group, a certain number of inflammatory cells, capillaries, collagen fibers and disordered arrangement were observed in the wounds of the diabetic+CNPS-PF group; the diabetic + TA-CNPS-PF group showed varying degrees of thin-walled capillary hyperplasia and collagen distribution, with fewer inflammatory cells at the trauma site, and more granulation tissues and blood vessels formed and no epidermal shape was present (Figure 3B and C). On Day 14, the diabetic + TA-CNPS-PF group presented a regenerated epidermis and dermis tissue structure, and the epidermis of the newborn granulation tissue was complete and thick; however, the diabetic group did not experience the above phenomenon, and there were still obvious inflammatory cells on Day 14. The regenerated epidermis and dermis structure of the control group was incomplete, and the collagen fibers were arranged irregularly. The diabetic + CNPS-PF group also presented regenerated epidermis. The regenerated epidermis and dermis in the control group were incomplete, and the collagen fibers were irregularly arranged; however, in the diabetes+CNPS-PF group, there was also a regenerated epidermis and dermis, but the collagen fibers were more sparsely arranged than those in the diabetes+TA-CNPS-PF group were (Figure 3B and C).

TAs Promote the Polarization of M1 Macrophages to M2 Macrophages

To clarify the mechanism by which TAs promote diabetic wound healing, we investigated the effect of TAs on macrophages. We established a diabetic cellular model by adding 40 mmol/L glucose in DMEM to cultured macrophages and then adding 2 μM TA to detect M1 macrophages and M2 macrophages (Figure 4A). First, the cytotoxicity (IC_{50} value) of TA to macrophages was 4.798 μM, which also demonstrated that 2 μM TA had no obvious effect on macrophages (Figure 4B). After the cellular diabetes model was established and the cytotoxicity (IC_{50} value) of TA was determined, we observed the morphological changes in the macrophages under a light microscope. The results revealed that the macrophage morphology in the high glucose + 2 μM TA group changed from round to pike (M2 macrophage morphology). A small number of pike-shaped macrophages were also observed in the TA group (2 μM TA), whereas the control and high glucose groups of cells were round in shape (Figure 4C). Staining for the M1 macrophage marker CD86 and the M2 macrophage marker CD206 revealed that high glucose induced M1 macrophages and that TA induced the polarization of M1 macrophages into M2 macrophages (Figure 4C). The effect of TA on macrophages was demonstrated by flow cytometry with Allophycocyanin (APC), a fluorescent dye that labels M2 macrophages with CD206, which revealed that 1.44% of the M2 macrophages in the control group, 2.58% of the M2 macrophages in the high glucose group, 14.61% of the M2 macrophages in the high glucose + 2 μM TA group and 10.55% of the M2 macrophages in the 2 μM TA group (Figure 4D and Supplementary Figure 2). Moreover, we selected the skin tissue of the trauma group on the 7th day for immunofluorescence with the M2 macrophage marker CD206. The results revealed that there were significantly more M2 macrophages in the TA-CNPS-PF group than in the CNPS-PF, DM and control groups, and the number of M2 macrophages in the diabetic group was lower than that in the control

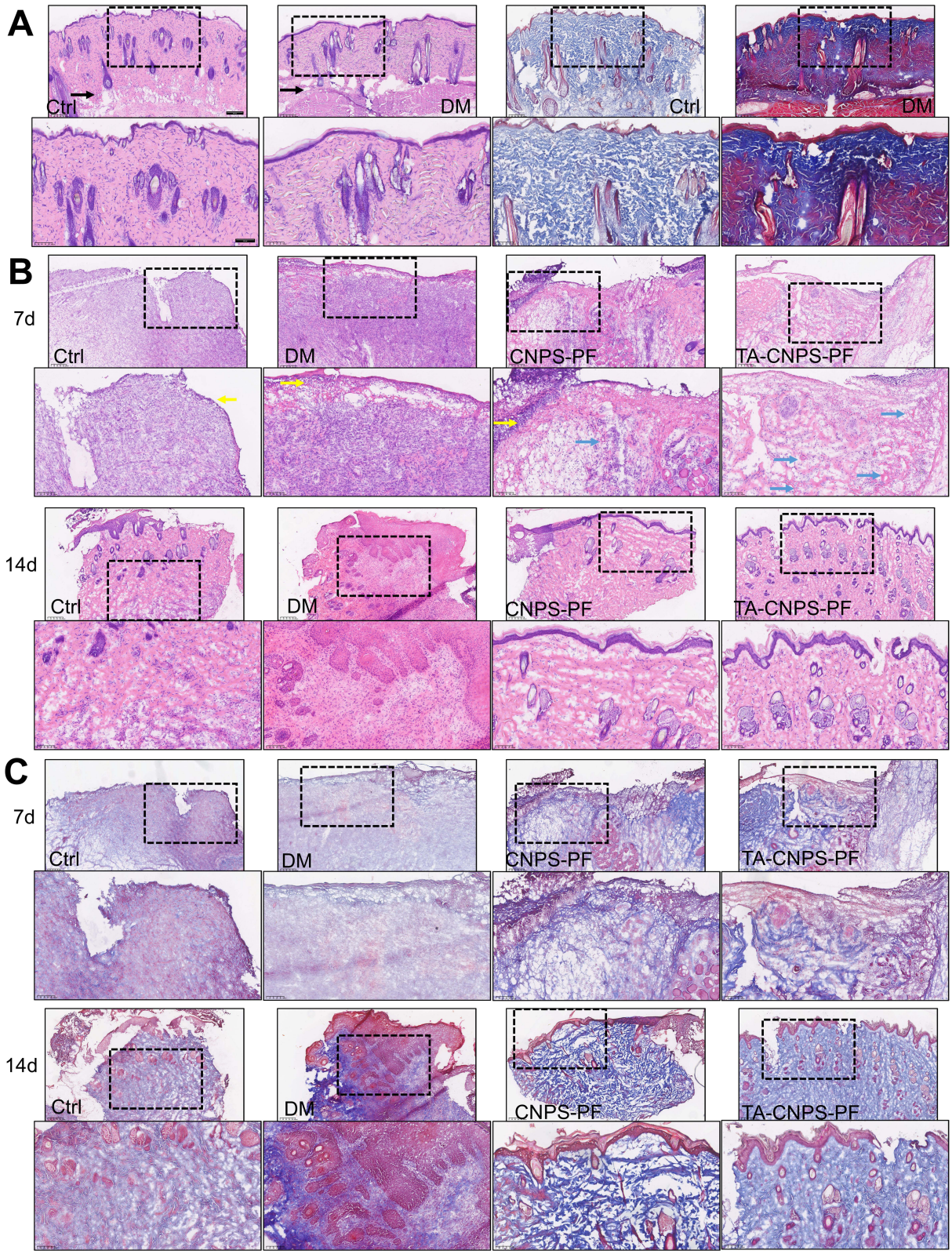

Figure 3 Histological analyses of regenerated skin tissues. (**A**) HE staining and Masson staining of microscopy images at 0 d. The dermis and fat layer of the skin in the control group were thicker than those in the diabetic group. The collagen fibers in the dermis of the control group were tighter and more regularly arranged than those in the dermis of the diabetic group. The black arrows indicate the fat layer in the samples. Magnified images of the corresponding area indicated by the black rectangular box (4×, 10×) (n=5); (**B**) Microscopy images of HE staining at 7 and 14 days. Blue arrows: neovascularization; yellow arrows: inflammatory cell infiltration; magnified images of the corresponding regional areas are indicated by black rectangular boxes (4×, 10×) (n=5). (**C**) Microscopy images of Masson staining at 7 and 14 days. Blue indicates collagen fibers, red indicates muscle fibers, and magnified images of the corresponding areas are indicated by the black rectangular box (4×,10×) (n=5). *P<0.05, **P < 0.01, ***P < 0.001, ****P < 0.0001.

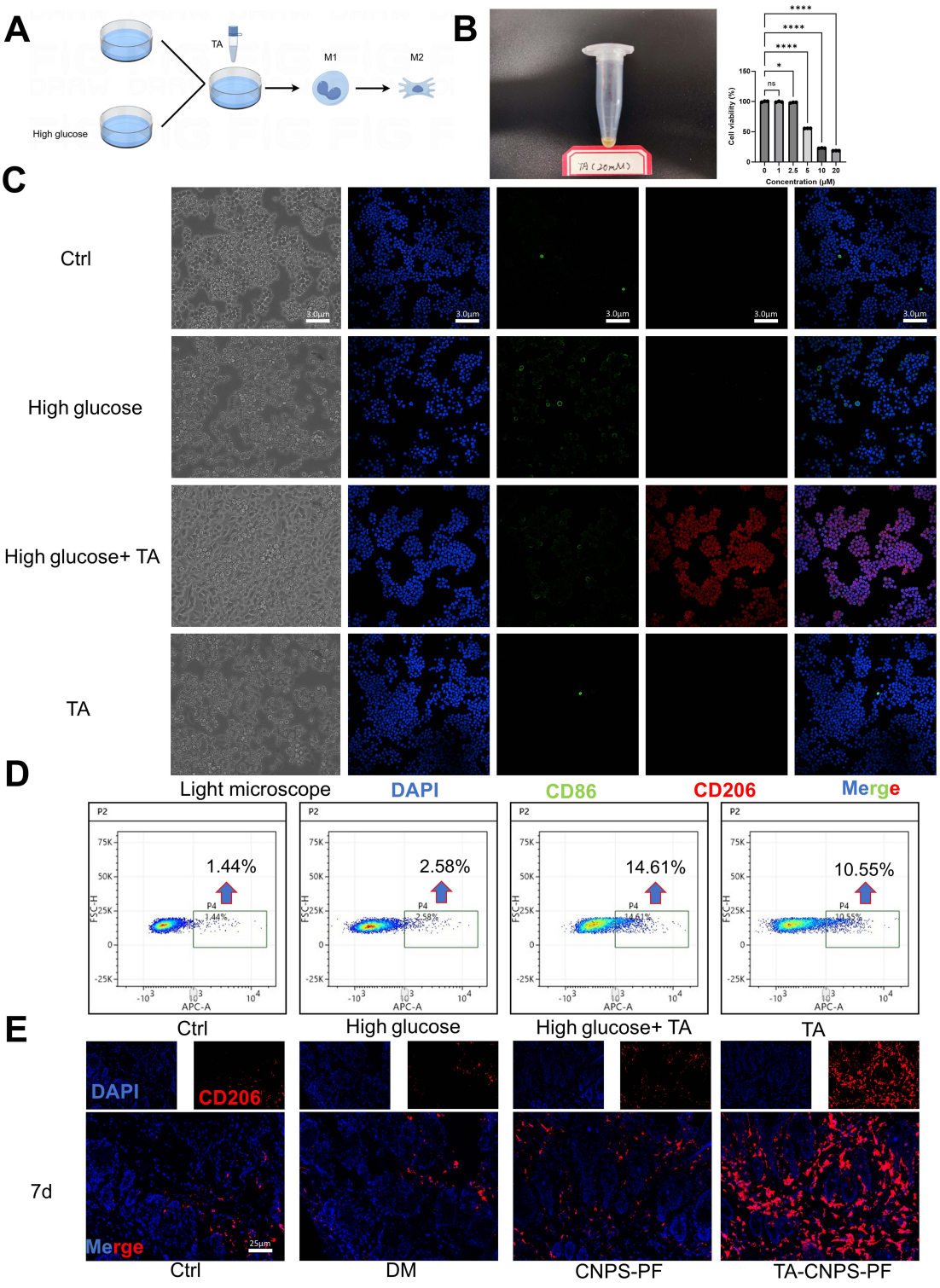

Figure 4 TAs promote the polarization of M1 macrophages into M2 macrophages. (**A**) Flowchart of the effects of TA on RAW264.7 cells; (**B**) Appearance of 20 mm TA and measurement of the effects of different concentrations of TA at 0, 1, 2.5, 5, 10, and 20 μM on RAW264.7 cells via the CCK8 assay. The cellular activity decreased with increasing TA concentration. The IC_{50} of TA on RAW264.7 cells was calculated, and the concentration of TA administered was determined to be 2 μM (n=3). (**C**) Light microscopy images of the control, high-glucose, high-glucose + 2 μM TA and 2 μM TA groups. The morphology of the macrophages in the high glucose+ 2 μM TA group changed from round to pike, and a small number of pike cells were observed in the 2 μM TA group. In the control and high-glucose groups, the cells were round (40×) (n=3). Immunocytometry of CD86 (green fluorescence, an M1 macrophage marker), CD206 (red fluorescence, an M2 macrophage marker), and nuclei (blue fluorescence, a nuclear marker) in the high-glucose group induced M1 macrophages, and TA induced the polarization of M1 macrophages into M2 macrophages (400 ×) (n=3). (**D**) Flow cytometry was used to detect the effect of TA on the expression of CD206. RAW264.7 cells in the M0 state were treated with 40 mmol/L glucose for 24 h in the presence of TA and labeled with an APC-coupled antibody against CD206 for flow cytometric analysis (n=3). (**E**) Immunofluorescence was used to detect the expression of CD206 in rat skin tissues on Day 7. CD206 (red fluorescence, M2 macrophage marker) and nuclei (blue fluorescence, nuclear marker) were detected (n=5). *P<0.05, **P < 0.01, ***P < 0.001, ****P < 0.0001.

and CNPS-PF groups (Figure 4E). Thus, TAs induced M2 macrophage polarization. These results indicate that diabetes induces M1 macrophages and that TAs promote the polarization of M1 macrophages into M2 macrophages to contribute to tissue repair at the wound site.

Discussion

Diabetes is a chronic disease, with its global prevalence among people aged 20–79 years estimated at 10.5% (536.6 million people) in 2021 and projected to rise to 12.2% (783.2 million people) in 2045. The global health expenditure related to diabetes was $966 billion in 2021 and is projected to reach $1054 billion by 2045.[29] The epidemic of diabetes and its complications poses a major threat to global health, reducing life expectancy[3,30,31] and increasing financial pressure.[29] Recently, studies on the mechanisms of diabetic wounds have focused on the following aspects: (1) induction of angiogenesis: local angiogenesis in diabetic wounds enhances keratinocyte differentiation as well as migration and re-epithelialization, increases the proliferation of fibroblasts and collagen synthesis and promotes wound contraction to increase the wound oxygen content;[32,33] (2) reducing the inflammatory response: reducing the levels of the proinflammatory cytokines IL-1β, IL-6 and TNF-α and increasing the levels of the anti-inflammatory factors IL-4, IL-10 and IL-13;[34] and (3) enhancing the extracellular matrix: the extracellular matrix consists of macromolecules that form a complex reticular dynamic structure that facilitates the transport of substances.[35]

In recent years, the treatment of diabetic wounds has included dressings, antibiotics to treat infections and hemodilution via peripheral arterial disease (PAD).[36] Currently, the main components of dressing therapy include the following: (1) growth factors and cytokines; (2) gene therapy: GAM501, PDGF-B gene; (3) extracellular matrix (ECM): A-cell keratinocyte skin grafts and porcine bladder matrices; (4) hydrogels: hydrogel dressings also protect wounds from microbial infections and promote effective healing; (5) mesenchymal stem cells; and (6) drugs containing botanical ingredients.[1] However, the quality of evidence available from published studies is insufficient to recommend any particular treatment or dressing product over any other. Finding a way to promote diabetic wound healing has become one of the key areas of current research.

Macrophages play a crucial role in wound healing.[37] Macrophages at the wound site, which stimulate angiogenesis, fibroproliferation and extracellular mesenchyme production, play important bridging roles in the transition of the wound from the inflammatory phase to the proliferative phase. During the inflammatory response in wounds, macrophages converge and differentiate into proinflammatory macrophages (M1) and anti-inflammatory macrophages (M2). M1 macrophages produce proinflammatory mediators such as TNF-α, IL-1 and IL-6. M2 macrophages are involved mainly in the downregulation of inflammation through the release of anti-inflammatory factors such as IL-4, IL-10 and IL-13. Therefore, promoting the polarization of M1 macrophages to M2 macrophages is beneficial for accelerating diabetic wound healing.[11] Xuelian Wei et al reported that the PAAc/CFCS-vanillin hydrogel promotes diabetic wound healing by promoting M2 macrophage polarization. However, this in vitro study demonstrated that PAAc/CFCS-vanillin reduced the expression of M1 biomarkers (including TNF-α, IL-1β and inducible nitric oxide synthase (iNOS)) and increased the expression of the M2 biomarkers IL-10, arginase-1 (Arg-1) and mannose receptor C-type 1 (MRC-1) via q–PCR.[38] In our study, Thonningianin A (TA) effectively promoted the polarization of M1 macrophages to M2 macrophages both in vivo and in vitro (Figure 4C, D and E).

Antimicrobial therapy is essential for accelerating the healing of diabetic wounds because their hyperglycemic environment is conducive to bacterial colonization. Studies have shown that chitosan has good hemostatic, antimicrobial, biocompatible and biodegradable properties.[21] In our study, TA-CNPS-PF exhibited the best antimicrobial performance among the tested groups. Controlled or sustained nanoparticle drug delivery systems enable maintenance of a constant drug concentration at the desired site.[17] Maintaining a constant drug concentration at the site of action is essential for diabetic wound treatment.[17] The preparation of nanoparticles with chitosan has been shown to improve drug stability and thereby increase drug accumulation.[22] The role of chitosan nanoparticles (CNPS) in promoting wound healing has been demonstrated.[22] In this study, encapsulating TA in chitosan nanoparticles for the treatment of wounds facilitated the control of TA release, maintained a constant concentration of TA at the wounds and improved the stability and utilization of TA (Figure 1D).

The relationship between antimicrobial agents and macrophage polarization warrants further investigation. Macrophages play a critical role in immune responses, with their polarized states significantly influencing inflammatory responses and pathogen clearance. Existing studies suggest that certain antimicrobial agents can modulate macrophage polarization, thereby affecting their functionality and cytokine production. Collagen sponge scaffolds loaded with Trichostatin A pretreated BMSCs-derived exosomes regulate macrophage polarization to promote skin wound healing.[39] Ph-responsive hyperbranched polymer nanoparticles to combat intracellular infection by disrupting bacterial wall and regulating macrophage polarization. However, research in this area remains limited.[40] Different antimicrobial agents may exhibit distinct mechanisms of action on macrophage polarization and the clinical relevance of these effects has not been thoroughly validated. Therefore, future research should focus on elucidating how various types of antimicrobial agents influence macrophage polarization and their overarching impact on immune responses. Understanding these interactions is crucial for optimizing antimicrobial treatment strategies and enhancing patient outcomes.

Studies have shown that keeping wounds moist is conducive to diabetic wound healing. Owing to their three-dimensional porous structure and high hydrophilicity, hydrogels can retain moisture in wounds, reduce bacterial infections and create a moist environment to promote wound healing.[37] Diabetic wounds are generally irregular wounds, which cannot be fit by traditional dressings; this means that the drug cannot uniformly cover the wound, resulting in poor wound healing. Owing to its unique thermal reversibility, a hydrogel is liquid at low temperature and gradually transforms into a semisolid gel at elevated temperatures so that the agent adheres to the target site and performs its biological role.

This study used a novel TA compound identified from the traditional Chinese medicinal herb *Penthorum chinense* Pursh, which is more economical, safer and more readily available than synthetic drugs. In this study revealed that TA promoted the polarization of M1 macrophages into M2 macrophages. Moreover, the use of chitosan and a hydrogel combined with TA to prepare a dressing system that could accommodate diabetic irregular wounds and antimicrobial and stable release of TA to promote diabetic wound healing. However, in this study, it investigated only the mechanism by which TAs affect macrophages in diabetic wounds, and whether TA drugs act on fibroblasts, vascular endothelial cells, etc, in diabetic wounds remains to be investigated. In addition, the penetration of drugs into tissues remains to be studied.

Conclusions

In this study, TA-CNPS-PF was developed successfully, which is considered an effective wound dressing for chronic diabetic wounds. TA-CNPS-PF effectively promoted wound healing by promoting the polarization of M1 macrophages to M2 macrophages. In all, TA-CNPS-PF has great potential for application in clinical diabetic chronic wound treatment, providing new ideas and an experimental basis for the use of traditional Chinese medicine and diabetic wound research.

Abbreviations

APC, Allophycocyanin; BSA, Bovine serum albumin; CCK8, Cell counting kit 8; CD206, Mannose Receptor; CD86, B-lymphocyte antigen B7-2; CNPS-PF, Chitosan nanoparticles composite PF-127 hydrogel; CS, Chitosan; DAPI, Propidium iodide; DM, Diabetes mellitus; DMSO, Dimethyl sulfoxide; *E. coli, Escherichia coli*; FBS, Fetal bovine serum; HE, Hematoxylin-eosin; NS, Normal saline; PBS, Phosphate buffer saline solution; PF-127, Pluronic(R) F-127; RAW264.7, Mouse Mononuclear Macrophages Cells; *S. aureus, Staphylococcus aureus*; STZ, Streptococcus aureus; TA, Thonningianin A; TA-CNPS-PF, Thonningianin A (TA)-loaded chitosan nanoparticles encapsulated by PF-127 hydrogel; TPP, Sodium tripolyphosphate; UV, Ultraviolet.

Funding

This study was supported by the National Natural Science Foundation of China (82470430), the International Science and Technology Innovation Cooperation Project of Sichuan Province (22GJHZ0278), the Sichuan Science and Technology Program (2022YFS0614), the Key Laboratory of Medical Electrophysiology (Southwest Medical University) Open fund (KeyME-2024-07), the Medical Research Project of Sichuan Province (S21020), the Science and Technology Strategic Cooperation Project of Luzhou Municipal People's Government and Southwest Medical University (2021LZXNYD-D10), and the Doctoral Research Initiation Program of the Affiliated Hospital of Southwest Medical University (19041).

Disclosure

The authors have no conflicts of interest to declare.

References

1. Pawar KB, Desai S, Bhonde RR, Bhole RP, Deshmukh AA. Wound with diabetes: present scenario and future. *Curr Diabetes Rev*. 2021;17(2):136–142.
2. Cole JB, Florez JC. Genetics of diabetes mellitus and diabetes complications. *Nat Rev Nephrol*. 2020;16(7):377–390. doi:10.1038/s41581-020-0278-5
3. Jeffcoate WJ, Vileikyte L, Boyko EJ, Armstrong DG, Boulton A. Current challenges and opportunities in the prevention and management of diabetic foot ulcers. *Diabetes Care*. 2018;41(4):645–652. doi:10.2337/dc17-1836
4. Patel S, Srivastava S, Singh MR, Singh D. Mechanistic insight into diabetic wounds: pathogenesis, molecular targets and treatment strategies to pace wound healing. *Biomed Pharmacother*. 2019;112:108615. doi:10.1016/j.biopha.2019.108615
5. Armstrong DG, Boulton A, Bus SA. Diabetic foot ulcers and their recurrence. *N Engl J Med*. 2017;376(24):2367–2375. doi:10.1056/NEJMra1615439
6. Liang Y, He J, Guo B. Functional hydrogels as wound dressing to enhance wound healing. *Acs Nano*. 2021;15(8):12687–12722. doi:10.1021/acsnano.1c04206
7. Zhang Y, Jiang W, Kong L, Fu J, Zhang Q, Liu H. Plga@il-8 nanoparticles-loaded acellular dermal matrix as a delivery system for exogenous MSCs in diabetic wound healing. *Int J Biol Macromol*. 2023;224:688–698. doi:10.1016/j.ijbiomac.2022.10.157
8. Huang C, Dong L, Zhao B, et al. Anti-inflammatory hydrogel dressings and skin wound healing. *Clin Transl Med*. 2022;12(11):e1094.
9. Anders CB, Lawton T, Ammons M. Metabolic immunomodulation of macrophage functional plasticity in nonhealing wounds. *Curr Opin Infect Dis*. 2019;32(3):204–209. doi:10.1097/QCO.0000000000000550
10. Yao Y, Xu XH, Jin L. Macrophage polarization in physiological and pathological pregnancy. *Front Immunol*. 2019;10:792. doi:10.3389/fimmu.2019.00792
11. He T, Sun P, Liu B, et al. Puffball spores improve wound healing in a diabetic rat model. *Front Endocrinol*. 2022;13:942549. doi:10.3389/fendo.2022.942549
12. Sun X, Wu A, Kwan LB, et al. The active components derived from penthorum chinensepursh protect against oxidative-stress-induced vascular injury via autophagy induction. *Free Radic Biol Med*. 2020;146:160–180. doi:10.1016/j.freeradbiomed.2019.10.417
13. Oksdath MM, Salazar-Hernandez C, Perrin SL, et al. 3d-printed microplate inserts for long term high-resolution imaging of live brain organoids. *Bmc Biomed Eng*. 2021;3(1):6. doi:10.1186/s42490-021-00049-5
14. Zheng B, Ye J, Yang Y, Huang Y, Xiao M. Self-healing polysaccharide-based injectable hydrogels with antibacterial activity for wound healing. *Carbohydr Polym*. 2022;275:118770.
15. Cha GD, Lee WH, Sunwoo S, et al. Multifunctional injectable hydrogel for in vivo diagnostic and therapeutic applications. *Acs Nano*. 2022;16(1):554–567. doi:10.1021/acsnano.1c07649
16. Lee Y, Hong Y, Wu T. Novel silver and nanoparticle-encapsulated growth factor co-loaded chitosan composite hydrogel with sustained antimicrobility and promoted biological properties for diabetic wound healing. *Mater Sci Eng C*. 2021;118:111385. doi:10.1016/j.msec.2020.111385
17. Bai Q, Han K, Dong K, et al. Potential applications of nanomaterials and technology for diabetic wound healing. *Int J Nanomed*. 2020;15:9717–9743. doi:10.2147/IJN.S276001
18. Fahimirad S, Abtahi H, Satei P, Ghaznavi-Rad E, Moslehi M, Ganji A. Wound healing performance of pcl/chitosan based electrospun nanofiber electrosprayed with curcumin loaded chitosan nanoparticles. *Carbohydr Polym*. 2021;259:117640.
19. Simões D, Miguel SP, Ribeiro MP, Coutinho P, Mendonça AG, Correia IJ. Recent advances on antimicrobial wound dressing: a review. *Eur J Pharm Biopharm*. 2018;127:130–141. doi:10.1016/j.ejpb.2018.02.022
20. Wroblewska M, Szymanska E, Winnicka K. The influence of tea tree oil on antifungal activity and pharmaceutical characteristics of pluronic((r)) f-127 gel formulations with ketoconazole. *Int J Mol Sci*. 2021;22(21):11326. doi:10.3390/ijms222111326
21. Deng Q, Huang S, Wen J, et al. Pf-127 hydrogel plus sodium ascorbyl phosphate improves wharton's jelly mesenchymal stem cell-mediated skin wound healing in mice. *Stem Cell Res Ther*. 2020;11(1):143.
22. Liu Z, Tang W, Liu J, et al. A novel sprayable thermosensitive hydrogel coupled with zinc modified metformin promotes the healing of skin wound. *Bioact Mater*. 2023;20:610–626. doi:10.1016/j.bioactmat.2022.06.008
23. Yang J, Chen Z, Pan D, Li H, Shen J. Umbilical cord-derived mesenchymal stem cell-derived exosomes combined pluronic f127 hydrogel promote chronic diabetic wound healing and complete skin regeneration. *Int J Nanomed*. 2020;15:5911–5926. doi:10.2147/IJN.S249129
24. Welz AN, Emberger-Klein A, Menrad K. Why people use herbal medicine: insights from a focus-group study in Germany. *Bmc Complement Altern Med*. 2018;18(1):92.
25. Bai Q, Gao Q, Hu F, et al. Chitosan and hyaluronic-based hydrogels could promote the infected wound healing. *Int J Biol Macromol*. 2023;232:123271. doi:10.1016/j.ijbiomac.2023.123271
26. Lutz TA. Mammalian models of diabetes mellitus, with a focus on type 2 diabetes mellitus. *Nat Rev Endocrinol*. 2023;19(6):350–360. doi:10.1038/s41574-023-00818-3
27. Lee KD, Chiang MH, Chen PH, et al. The effect of low-level laser irradiation on hyperglycemia-induced inflammation in human gingival fibroblasts. *Lasers Med Sci*. 2019;34(5):913–920. doi:10.1007/s10103-018-2675-6
28. Kim IS, Park HC, Quan H, Kim Y, Wu L, Yang HC. Effects of triethylene glycol dimethacrylate and hydroxyethyl methacrylate on macrophage polarization. *Int Endod J*. 2019;52(7):987–998. doi:10.1111/iej.13088
29. Sun H, Saeedi P, Karuranga S, et al. Idf diabetes atlas: global, regional and country-level diabetes prevalence estimates for 2021 and projections for 2045. *Diab Res Clin Pract*. 2022;183:109119. doi:10.1016/j.diabres.2021.109119
30. Heald AH, Stedman M, Davies M, et al. Estimating life years lost to diabetes: outcomes from analysis of national diabetes audit and office of national statistics data. *Cardiovasc Endocrinol Metab*. 2020;9(4):183–185.
31. Zheng Y, Ley SH, Hu FB. Global aetiology and epidemiology of type 2 diabetes mellitus and its complications. *Nat Rev Endocrinol*. 2018;14(2):88–98. doi:10.1038/nrendo.2017.151

32. Ndip A, Ebah L, Mbako A. Neuropathic diabetic foot ulcers - evidence-to-practice. *Int J Gen Med*. 2012;5:129–134. doi:10.2147/IJGM.S10328
33. Rodriguez PG, Felix FN, Woodley DT, Shim EK. The role of oxygen in wound healing: a review of the literature. *Dermatol Surg*. 2008;34 (9):1159–1169.
34. Yoshida S, Koshima I, Hamada Y, et al. Lymphovenous anastomosis aids wound healing in lymphedema: relationship between lymphedema and delayed wound healing from a view of immune mechanisms. *Adv Wound Care*. 2019;8(6):263–269. doi:10.1089/wound.2018.0871
35. Sutherland TE, Dyer DP, Allen JE. The extracellular matrix and the immune system: a mutually dependent relationship. *Science*. 2023;379(6633). doi:10.1126/science.abp8964
36. Wu L, Norman G, Dumville JC, O'Meara S, Bell-Syer SEM. Dressings for treating foot ulcers in people with diabetes: an overview of systematic reviews. *Cochrane Database Syst Rev*. 2015;7. CD10471. doi:10.1002/14651858.CD001555.pub5
37. Farahani M, Shafiee A. Wound healing: from passive to smart dressings. *Adv Healthc Mater*. 2021;10(16):e2100477. doi:10.1002/adhm.202100477
38. Wei X, Liu C, Li Z, Gu Z, Yang J, Luo K. Chitosan-based hydrogel dressings for diabetic wound healing via promoting m2 macrophage-polarization. *Carbohydr Polym*. 2024;331:121873.
39. Wang T, Xue Y, Zhang W, Zheng Z, Peng X, Zhou Y. Collagen sponge scaffolds loaded with trichostatin a pretreated bmscs-derived exosomes regulate macrophage polarization to promote skin wound healing. *Int J Biol Macromol*. 2024;269:131948. doi:10.1016/j.ijbiomac.2024.131948
40. Yang L, Dai X, Xu Q, Li Y, Liu X, Gao F. Ph-responsive hyperbranched polymer nanoparticles to combat intracellular infection by disrupting bacterial wall and regulating macrophage polarization. *Biomacromolecules*. 2022;23(10):4370–4378. doi:10.1021/acs.biomac.2c00823